Excitation of multiple giant dipole resonances: from spherical to deformed nuclei

M.V. Andrés [a], E.G. Lanza [a,b], P. Van Isacker [c], C. Volpe [d], F. Catara [b]

[a] *Departamento de Física Atómica, Molecular y Nuclear, Universidad de Sevilla, Apdo 1065, 41080 Sevilla, Spain*
[b] *Dipartimento di Fisica dell'Università and INFN, Sezione di Catania, I-95129 Catania, Italy*
[c] *GANIL, BP 5027, F-14076 Caen Cedex 5, France*
[d] *Groupe de Physique Théorique, Institut de Physique Nucléaire, F-91406 Orsay Cedex, France*

Abstract

The effect of deformation on the excitation of multiple giant dipole resonances is studied. Analytical expressions are derived in the framework of the interacting boson model for the energies and E1 properties of giant dipole resonances in spherical and deformed nuclei, and a numerical treatment of transitional nuclei is proposed. Coulomb-excitation cross sections are calculated in ^{238}U and in the samarium isotopes. © 1999 Published by Elsevier Science B.V. All rights reserved.

Nuclear multiphonons both at low and at high energies have attracted much interest lately [1–4]. At low energy, the controversy centers around the collective character of multiphonon states. While in vibrational nuclei firm experimental evidence now exists for states with triple quadrupole phonon character (see, e.g., Ref. [5]), in deformed nuclei the collective character of double β and γ vibrations is still a matter of acrimonious debate. At high energy, the study of multiphonons has pointed out the limitations of the small-amplitude approximation for vibrational collective motion and of the linear approximation for the external exciting field. These assumptions are routinely made for the first phonon but recent studies of double phonons [6–8] have shown the importance of anharmonicities and non-linearities in the excitation of large-amplitude vibrations. Similarly, anharmonicities and non-linearities in nuclear vibrations at low energy have been shown to play a crucial role in the calculation of the heavy-ion fusion cross sections at energies close to the Coulomb barrier [9,10].

In this letter yet another aspect of phonon excitations at high energy is investigated, namely the modification of the excitation of the giant dipole resonance (GDR) away from shell closure as a result of deformation. Already at the level of the single GDR the strength function shows a splitting into two peaks associated with the two different frequencies of vibration along with or perpendicular to the axis of axial symmetry. The question under scrutiny here is how deformation influences the E1 strength to the double GDR (DGDR) and what its effect is on the Coulomb excitation cross section. The proposed approach makes use of the interacting boson model (IBM) [11] for the description of the low-energy collective levels. These are coupled to the GDR excitations modelled as p bosons. The advantage of

using the IBM is that the multiphonon states are obtained as exact eigensolutions of the hamiltonian and, therefore, no folding procedure is required to obtain the double phonon states, as is for instance the case in Refs. [12,13]. The folding procedure is only approximately correct for vibrational or well-deformed nuclei (in the latter case the folding must be done in the intrinsic frame assuming additivity of intrinsic phonons) but there is no simple recipe in the intermediate case of transitional nuclei. Another advantage of the IBM is that calculations are quick and this enables an easy estimate of the excitation cross section to the triple GDR concerning which experiments are currently planned [14].

A general and appropriate basis to discuss the problem of multiple GDR excitations is of the form

$$|\alpha_L L \times nR; JM_J\rangle. \tag{1}$$

The multiple GDR is built on a low-energy nuclear state characterised by $\alpha_L L$ where L is the angular momentum of the state and α_L any other label. The multiplicity of the GDR is indicated by n (i.e., $n = 1$ for a single GDR, $n = 2$ for a double GDR, etc.) and its angular momentum by R. The single resonance is approximated as a p boson; the allowed angular momenta of the multiple GDR are $R = n, n-2, \ldots, 0$ or 1. The basis (1) can be referred to as a *weak-coupling basis* in the sense that the angular momenta L and R are good quantum numbers and are coupled to total angular momentum J with projection M_J. The weak-coupling basis arises naturally when the interaction between the GDR and the low-lying states is weak or is of dipole type $\hat{L} \cdot \hat{R}$. More general nuclear interactions are not necessarily diagonal in the basis (1). Specifically, the interaction predominantly responsible for the splitting of the GDR in deformed nuclei is of quadrupole type $\hat{Q}_L \cdot \hat{Q}_R$ and is not diagonal in the weak-coupling basis (1). From the analogous problem in the particle–core coupling model [15] it is known that the diagonalisation of $\hat{Q}_L \cdot \hat{Q}_R$ in the basis (1) gives rise to a *strong-coupling basis* with the quantum numbers [16]

$$|\alpha_L \times n; \alpha_J K_J JM_J\rangle. \tag{2}$$

The angular momenta L and R no longer are conserved quantities and are replaced by K_J, the projection of the total angular momentum J on the axis of axial symmetry. The choice of basis depends on the competition between various terms in the nuclear hamiltonian. Large splittings in L or R induce the weak-coupling basis (1); if, in contrast, these are small in comparison with the quadrupole coupling between the low-energy states and the GDR, such as is the case in well-deformed nuclei, the strong-coupling basis (2) is obtained.

The above remarks are rather general and model independent. Low-energy nuclear states and their coupling with the GDR can be modelled in several different ways and a convenient one is in the context of the IBM [11,17]. In deformed nuclei the problem was worked out analytically for a single GDR by Rowe and Iachello [18], while numerical results were presented for the single GDR in Refs. [19–22] and later for the double GDR in Ref. [23]. In this letter analytical results for the energies and E1 transitions in spherical and deformed nuclei are generalised to the multiple GDR, and numerical results are presented for intermediate cases. From these results the Coulomb-excitation cross-sections are calculated taking into account the dynamics of the collision, which was lacking in previous IBM treatments of the single and the double GDR.

It is assumed in the IBM that collective nuclear states can be described in terms of N, s and d bosons where N is half the number of valence nucleons [11]. The dynamical algebra of the model is U(6) in the sense that a single of its representations (namely the symmetric one, $[N]$) is assumed to contain all low-energy collective nuclear states. To this space are coupled the multiple GDR excitations. Assuming that a single GDR is described by a p boson, multiple GDR excitations are represented by the direct sum $(0,0) \oplus (1,0) \oplus (2,0) \oplus \cdots$ of symmetric representations $(n,0)$ of U(3). The dynamical algebra of the coupled system is thus U(6) $\otimes$ U(3) with the proviso that several U(3) representations must be taken to build the model space.

The model hamiltonian has the generic form [17]

$$\hat{H} = \hat{H}_{sd} + \hat{H}_p + \hat{V}_{sd-p}. \tag{3}$$

The first term is the usual IBM hamiltonian [11] which gives an adequate description of the low-energy spectrum of spherical, deformed and transitional

nuclei. The second term in (3) governs the multiple GDR spectrum and is of the form

$$\hat{H}_p = \epsilon_p \hat{n} + \alpha_p \hat{n}(\hat{n} + 3) + \beta_p \hat{R}^2, \tag{4}$$

where $\hat{n}$ is the p-boson number operator and $\hat{R}$ the associated angular momentum operator. The coefficient ϵ_p represents the unperturbed single GDR energy. The second term in (4) induces a diagonal anharmonicity in the excitation energy of the multiple GDR. The interaction term in (3), finally, acquires the form

$$\hat{V}_{sd-p} = \alpha_0 \hat{n}_d \hat{n} + 2\alpha_1 \hat{L} \cdot \hat{R} + 2\sqrt{3}\,\alpha_2 \hat{Q}_L \cdot \hat{Q}_R, \tag{5}$$

with a monopole, dipole and quadrupole interaction. More complicated, higher-order interactions that mix excitations with different n are not included here. The hamiltonian (3) can be diagonalised numerically in the U(6) ⊗ U(3) model space. For particular values of the parameters analytical solutions are available. Two classes of analytically solvable hamiltonians exist.

(i) Weak-coupling limit. A weak-coupling hamiltonian can be defined for each of the three limits [U(5), SU(3) and O(6)] of the IBM and is obtained for $\alpha_0 = \alpha_2 = 0$ in (5). In the particular case of the U(5) limit, only $\alpha_2 = 0$ is required. In the U(5) weak-coupling limit states are labelled by

$$|[N]n_d v n_\Delta L \times (n,0) R; JM_J\rangle, \tag{6}$$

where n_d is the number of d bosons, v the d-boson seniority and n_Δ an additional quantum number related to the pairing of triplets of d bosons [11,25]. The energy eigenvalues of the states (6) are

$$\begin{aligned}
E &= \epsilon_d n_d + \alpha_d n_d (n_d + 4) \\
&\quad + \gamma_d v(v + 3) \\
&\quad + (\beta_d - \alpha_1) L(L + 1) + \epsilon_p n + \alpha_p n(n + 3) \\
&\quad + (\beta_p - \alpha_1) R(R + 1) \\
&\quad + \alpha_0 n_d n + \alpha_1 J(J + 1),
\end{aligned} \tag{7}$$

where β_d is the parameter associated with $\hat{L}^2$ in $\hat{H}_{sd}$.

(ii) Strong-coupling rotational limit. The appropriate classification of the low-energy states in this case is SU(3). This symmetry requires that the quadrupole operator $\hat{Q}_L$ be a generator of SU(3) and that $\alpha_0 = 0$ and $\beta_p = \beta_d = \alpha_1 - \frac{3}{4}\alpha_2$, In the SU(3) strong-coupling limit states are labelled by

$$|[N](\lambda_{sd}, \mu_{sd}) \times (n,0); (\lambda,\mu) K_J JM_J\rangle. \tag{8}$$

The labels (λ_{sd}, μ_{sd}) are associated with the SU(3) algebra of the s and d bosons. They characterise the band structure of the low-energy spectrum; for example, the ground band has $(\lambda_{sd}, \mu_{sd}) = (2N,0)$. The energy eigenvalues of the states (8) are

$$\begin{aligned}
E &= (\alpha_{sd} - \alpha_2) \\
&\quad \times [\lambda_{sd}(\lambda_{sd} + 3) + \mu_{sd}(\mu_{sd} + 3) + \lambda_{sd}\mu_{sd}] \\
&\quad + \epsilon_p n + (\alpha_p - \alpha_2) n(n + 3) \\
&\quad + \alpha_2 [\lambda(\lambda + 3) + \mu(\mu + 3) + \lambda\mu] \\
&\quad + (\alpha_1 - \tfrac{3}{4}\alpha_2) J(J + 1). \tag{9}
\end{aligned}$$

The splitting of the GDR comes about because of the fourth term in (9). The (GDR)^n excitation splits into $n + 1$ peaks corresponding to (λ,μ) values

$$\begin{aligned}
(\lambda,\mu) \\
= (2N + n,0), (2N + n - 2,1), \ldots, (2N - n,n),
\end{aligned} \tag{10}$$

where $2N \geq n$ is assumed. The energies of the different peaks are found from (9). The values of K_J and J allowed for a given (λ,μ) representation are given by Elliott's rule [11,24].

The Coulomb excitation of GDRs occurs predominantly through E1. In the context of the present model an E1 excitation corresponds to the creation of a p boson (annihilation in case of E1 de-excitation) and thus the electric multipole operator $\mathcal{M}(E1\mu)$ [15] is parametrised as $\zeta(p_\mu^\dagger + \tilde{p}_\mu)$. The calculation of E1 transition probabilities requires the matrix elements of $p^\dagger$ in the basis (6) or (8) which can be done by standard group-theoretical techniques. Analytical expressions are found in the two limiting cases.

(i) Weak-coupling limit. For the GDR excitations built on the 0^+ ground state results up to the DGDR are shown in Fig. 1a. Generally, for the B(E1) values between multipole GDR excitations built on
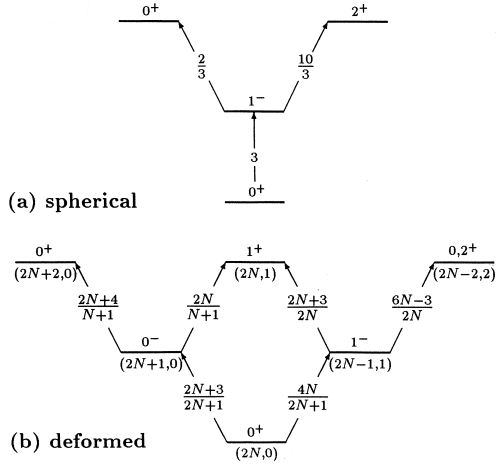
Fig. 1. E1 excitation patterns up to $(GDR)^2$ in (a) the spherical weak-coupling limit and (b) the deformed strong-coupling limit. (a) The levels are labelled by J^π on top. The numbers between levels are the strengths $B(E1;(n,0)J \to (n+1,0)J')$ in units of ζ^2. (b) The levels are labelled by (λ,μ) underneath and by K^π on top. The expressions between levels are the summed strengths $\sum_{K'L'} B(E1;(\lambda,\mu)KL \to (\lambda',\mu')K'L')$ in units of ζ^2.

the 0^+ ground state one recovers the independent-quanta result [15]

$$\sum_f B\left(E1; n_d = 0 \times (n,0) R_i = J_i; J_i \right.$$

$$\to n_d = 0 \times (n-1,0) R_f = J_f; J_f \right)$$

$$= \sum_f B\left(E1; \alpha n J_i \to \alpha (n-1) J_f \right)$$

$$= n B(E1; \alpha n = 1 \to \alpha n = 0), \qquad (11)$$

where α denotes all other quantum numbers that cannot change.

(ii) Strong-coupling rotational limit. Results up to the DGDR are shown in Fig. 1b. Although all individual $B(E1)$s are known, for simplicity of presentation only the summed strengths $\sum_{K'L'} B(E1;(\lambda,\mu)KL \to (\lambda',\mu')K'L')$ are shown. In the limit of large boson number N one recovers harmonic results that have a simple geometric interpretation. For example, the $B(E1)$ values from the 0^+ ground state to the two 1^- GDRs are 1 and 2, respectively, the first associated with an oscillation along the axis of sym-

metry (say the z direction) and the second with oscillations in the x and y directions. For the single-to-double GDR excitation one finds $B(E1)$ values which are, for $N \to \infty$, 2, 2, 1 and 3. The large-N results can be generalised to $(GDR)^n$.

Coulomb excitation in heavy-ion collisions is usually described by treating the relative motion classically while the internal degrees of freedom of the colliding nuclei are accounted for quantum mechanically. The operator responsible for the excitation depends on time through the relative distance. For relativistic collisions its expression is as in Eq. (35) of Ref. [7] where each term of the multiple expansion of the external field factorizes into two elements. The first depends on the collision properties, the second on the structure of the nucleus being excited. In the present study only contributions from the $\mathscr{M}(E1)$ matrix elements are considered and those are calculated within the model described above. The solution of the time-dependent Schrödinger equation leads to a set of coupled differential equations for the probability amplitudes to excite the $(GDR)^n$ states. For each impact parameter b these equations are integrated along the appropriate classical trajectory. For each $(GDR)^n$ state the total inelastic cross section is then obtained by integrating the corresponding probability over all impact parameters, starting from a mininum value $b_{min} = 1.34[A_1^{1/3} + A_2^{1/3} - 0.75(A_1^{-1/3} + A_2^{-1/3})]$ fm [26].

The above formalism will now be applied to the relativistic Coulomb excitation of the single and double GDRs in ^{238}U and in the chain of even isotopes ^{148}Sm to ^{154}Sm. The former is an example of a well-deformed nucleus while the samarium isotopes exhibit a change from vibrational to deformed as A increases. The description of such structural changes requires the use of a transitional IBM hamiltonian and hence the following analysis is not confined to any of the previously discussed analytical limits but always involves a numerical diagonalisation. For ^{238}U, a consistent-Q [27] hamiltonian $\hat{H}_{sd} = \kappa \hat{Q}^\chi \cdot \hat{Q}^\chi + \kappa' \hat{L} \cdot \hat{L}$ is used with $\kappa = -16$ keV, $\kappa' = 1.5$ keV and $\chi = -0.72$. These parameters yield an adequate description of the ground–gamma band splitting, of the moments of inertia and of the E2 transitions from gamma to ground band. The $\hat{H}_{sd}$ hamiltonian for the Sm isotopes is taken as in Ref. [21]. The additional parameters ϵ_p, α_0, α_2 and ζ in

$\hat{H}_p$, $\hat{V}_{sd-p}$ and in the E1 operator are given in Table 1. They have been chosen as to reproduce the observed photoabsorption cross section [28,29] to the first GDR. Agreement is obtained if to each eigenstate is associated a spreading width $\Gamma_i = 0.007E_i^{2.5}$ in ^{238}U and $\Gamma_i = 0.029E_i^{1.81}$ in the Sm isotopes (with E_i and Γ_i in MeV). To reproduce the photoabsorption cross section of a well-deformed nucleus one uses the fact that the energy splitting of the GDR is very sensitive to the parameter α_2. Then, once α_2 is fixed, one varies α_0 to sligthly change the contribution of each peak to the energy-weigthed sum rule and ϵ_p to shift the energy of the dipole states. Finally, the parameter ζ is obtained from a global normalisation.

Recently, an experiment was done for ^{238}U + ^{208}Pb at 0.5 GeV/A (the data analysis is in progress [30]). The result of the corresponding calculation is shown in Fig. 2. The full line corresponds to the total cross section obtained by smoothing the cross section to each discrete state with a Lorentzian having a width of $\Gamma_1 = 2.5$ MeV and $\Gamma_2 = \sqrt{2}\,\Gamma_1$ for the single and double GDR states, respectively. As expected, the GDR peak is split in two while a broad plateau occurs in the DGDR region. The integrated cross sections are $\sigma^{GDR} = 3.5$ b and $\sigma^{DGDR} = 0.3$ b, lower than those of Ponomarev et al. [13]. The difference can be ascribed to the fact that a coupled-channel method is used while in Ref. [13] the cross sections are calculated in first- and second-order perturbation theory. In fact, if we use perturbation theory then the result for the σ^{GDR} increases up to 4.2 b. The two approaches give similar results only for large impact parameters. Some difference comes also from the different $B(E1)$ distribution. Fig. 2 also shows the contributions associated with the 0^+ (dashed line) and 2^+ (dot-dashed line) component of
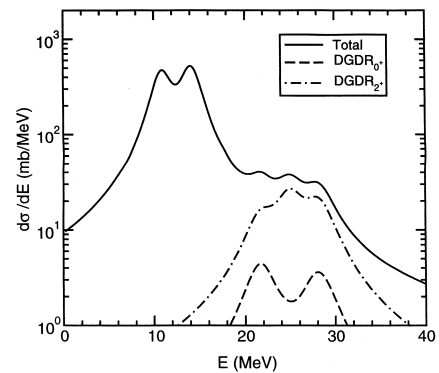

Fig. 2. Coulomb excitation of the single and double GDR in ^{238}U in the ^{238}U (0.5 GeV/A) + ^{208}Pb reaction. The dashed line is the contribution from the 0^+ component of the two-phonon state while the 2^+ one is represented by the dot–dashed line. The results corresponding to the 1^+ component are too small to be seen.

the DGDR. The 1^+ component does not appear in the figure since it is extremely small. After substraction of the long single GDR tail, the three peaks, expected from (10), are clearly visible. (If the convolution of the cross section were done with a $\Gamma_2 = 2\Gamma_1$, the three peaks are still visible though less evident). Therefore, an exclusive experiment in coincidence with γ–γ decay might conceivably give a direct signature of the excitation of the DGDR.

The present results differ from those of Ponomarev et al. [13] who study the same reaction with the particle–phonon model, using second-order perturbation theory to calculate the cross section. In Ref. [13] the DGDR cross section appears as a structureless peak while here it does not. The reason is that the calculated cross section to the single GDR in Ref. [13] shows three peaks in the energy region 11–15 MeV. As a result, since the DGDR states are constructed as products of two single GDR states, one expects six peaks in the DGDR energy region which eventually smear out the cross section to the DGDR. In our case we have only two peaks, which are present in the experimental data, because we have fixed the parameters of our hamiltonian by fitting the photoabsorption cross section.

The results of the calculated inelastic cross sections for the reactions ^{208}Pb + ^{A}Sm at 0.5 GeV/A are shown in Fig. 3. The cross sections to each

Table 1
Parameters of the hamiltonian and of the E1 transition operator

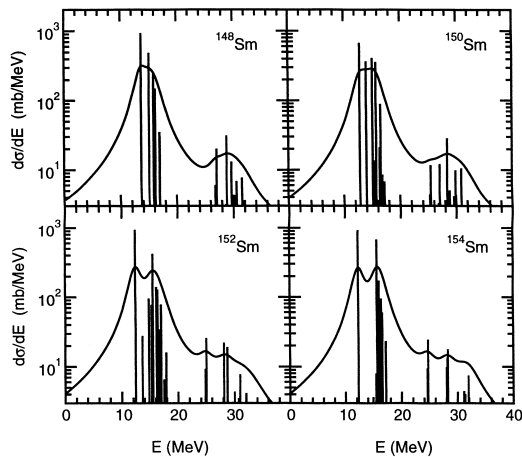| Isotope	ϵ_p (MeV)	α_0 (keV)	$2\sqrt{3}\,\alpha_2$ (keV)	ζ (e fm)
^{148}Sm	14.84	0	-275	3.84
^{150}Sm	14.59	0	-275	3.84
^{152}Sm	14.05	250	-275	3.84
^{154}Sm	13.99	150	-225	3.84
^{238}U	13.00	0	-160	5.06

Fig. 3. Coulomb excitation cross sections of single and double GDR in several samarium isotopes in the ^{208}Pb (0.5 GeV/A) + ^{A}Sm reaction. The bars correspond to the cross sections to the discrete states and the full line corresponds to the convolution of these cross sections by a lorentzian of width $\Gamma_1 = 2.5$ MeV for the one-phonon states and $\Gamma_2 = \sqrt{2}\,\Gamma_1$ for the two-phonon states.

discrete state are shown as well as the ones obtained by the same smoothing procedure described above. In the transition from spherical to deformed one observes a continous evolution in the shape of the cross section resulting in the deformed case in a clear splitting in two peaks of the GDR and, correspondingly, three bumps in the DGDR energy region. This effect is due to the increase in separation between the two main components of the single GDR and the concentration of the small components in a more narrow energy range which in turn results from the increasing coupling of the GDR with quadrupole modes.

In summary, energy and E1 properties of multiple giant dipole resonances have been studied in the context of the interacting boson model. The model has been applied to ^{238}U and to transitional samarium isotopes for which Coulomb excitation cross sections have been calculated in the reaction with ^{208}Pb at 0.5 GeV/A. The example of the samarium isotopes shows how the excitation cross section is modified when going from spherical to deformed nuclei. The calculation shows also that exclusive experiments on a well-deformed nucleus like ^{238}U could give a direct signature of the existence of the double giant dipole resonance.

Acknowledgements

References

[1] H. Emling, Prog. Part. Nucl. Phys. 33 (1994) 729.

[2] Ph. Chomaz, N. Frascaria, Phys. Rep. 252 (1995) 275.

[3] T. Aumann, P.F. Bortignon, H. Emling, Ann. Rev. Nucl. Part. Sci. 48 (1998) 351.

[4] X. Wu, A. Aprahamian, S.M. Fischer, W. Reviol, G. Liu, J.X. Saladin, Phys. Rev. C 49 (1994) 1837.

[5] M. Délèze, S. Drissi, J. Jolie, J. Kern, J.P. Vorlet, Nucl. Phys. A 554 (1993) 1.

[6] C. Volpe, F. Catara, Ph. Chomaz, M.V. Andrés, E.G. Lanza, Nucl. Phys. A 589 (1995) 521.

[7] E.G. Lanza, M.V. Andrés, F. Catara, Ph. Chomaz, C. Volpe, Nucl. Phys. A 613 (1997) 445.

[8] E.G. Lanza, M.V. Andrés, F. Catara, Ph. Chomaz, C. Volpe, Nucl. Phys. A 636 (1998) 452.

[9] K. Hagino, N. Takigawa, M. Dasgupta, D.J. Hinde, J.R. Leigh, J. Phys. G 23 (1997) 1413.

[10] K. Hagino, S. Kuyucak, N. Takigawa, Phys. Rev. C 57 (1998) 1349.

[11] F. Iachello, A. Arima, The Interacting Boson Model, Cambridge University Press, Cambridge, 1987.

[12] V.Yu. Ponomarev et al., Phys. Rev. Lett. 72 (1994) 1168.

[13] V.Yu. Ponomarev, C.A. Bertulani, A.V. Sushkov, Phys. Rev. C 58 (1998) 2750.

[14] N. Frascaria, private communication.

[15] A. Bohr, B.R. Mottelson, Nuclear Structure. I and II, Benjamin, Reading, 1975.

[16] D.M. Brink, B. Buck, R. Huby, M.A. Nagarajan, N. Rowley, J. Phys. G 13 (1987) 629.

[17] F. Iachello, P. Van Isacker, The Interacting Boson–Fermion Model, Cambridge University Press, Cambridge, 1991.

[18] D.J. Rowe, F. Iachello, Phys. Lett. B 130 (1983) 231.

[19] I. Morrison, J. Weise, J. Phys. G 8 (1982) 687.

[20] F.G. Scholtz, F.J.W. Hahne, Phys. Lett. B 123 (1983) 147.

[21] G. Maino, A. Ventura, L. Zuffi, F. Iachello, Phys. Rev. C 30 (1984) 2101.

[22] L. Zuffi, P. Van Isacker, G. Maino, A. Ventura, Nucl. Instr. Meth. Phys. Res. A 255 (1987) 46.

[23] F.G. Scholtz, F.J.W. Hahne, Z. Phys. A 336 (1990) 145.

[24] J.P. Elliott, Proc. R. Soc. (London) A 245 (1958) 562.

[25] O. Castaños, E. Chacón, A. Frank, M. Moshinsky, J. Math. Phys. 20 (1979) 35.

[26] C.J. Benesh, B.C. Cook, J.P. Vary, Phys. Rev. C 40 (1989) 1198.

[27] D.D. Warner, R.F. Casten, Phys. Rev. C 28 (1983) 1798.

[28] G.M. Gurevich et al., Nucl. Phys. A 273 (1976) 326; A. Veyssiere et al., Nucl. Phys. A 119 (1973) 45; J.T. Caldwell et al., Phys. Rev. C 21 (1980) 1215.

[29] P. Carlos et al., Nucl. Phys. A 225 (1974) 171.

[30] H. Emling, private communication.